

# IMPROVEMENT OF THE MAXIMUM FIELD OF ACCELERATING CAVITIES BY DRY OXIDATION.

R. Ballantini, A. Daccà, G. Gemme, R. Parodi<sup>#</sup>, INFN Sezione di Genova, Via Dodecaneso 33 16146 Genova Italy, L. Mattera, Unità INFN e Dipartimento di Fisica, Via Dodecaneso 33 16146 Genova Italy

## *Abstract*

Surface analysis by XPS and Auger spectroscopy on RF Grade Niobium showed a very strong dependence of the niobium surface layer to the content of water in the surface treatments. The water, detected as an OH+ chemical radical in the composition of the detected oxygen line of the XPS spectra, affects mainly the niobium oxide layer on the top of the surface. Niobium samples exposed to air (containing a 50 to 70% of water vapor) showed a thicker and less uniform oxide layer than Niobium samples exposed to DRY oxygen for the same amount of time. The oxide layer grown in air is in some extent porous, allowing the atmospheric oxygen to migrate through the oxide layer producing a thicker layer of oxidized Niobium. Some significant difference was also found in the value of the electronic work function. Last the dry grown surface layers are by far less reactive when exposed to air, even for some weeks, resulting in a lower contamination by the carbon, found on the niobium surface as graphite and Niobium carbide. As a result of our analysis we come to the conclusion that dry oxidized niobium surfaces will perform better in S/C cavities at high field, reducing both the residual losses and the field emitted current of NREL electrons. To check our hypothesis we extensively tested a 3 GHz cavity built using RRR 250 Niobium. After the usual deep chemical polishing (200 microns) the cavity reached 15 MV/m of accelerating field. A UHV firing at 1950 C improved the maximum field to 20 MV/m. In both the cavity runs the final limitation was a quite strong NREL. After the measurement the cavity was UHV fired again following the same schedule of the previous treatment. After the firing the cavity was exposed to dry oxygen. The limiting field increased to 32 MV/m without any detectable electron loading.

## 1 INTRODUCTION

The main aim of research in RF superconductivity is to reach the highest accelerating field with the lowest power dissipation inside the resonant cavities. It is now well recognised that RF performances are strongly related to the surface state of the cavities and, for this reason, a great effort is devoted to develop new surface

treatments and to characterise the new treated Nb cavities by surface analysis.

This paper shows the results of a study that was performed both on the side of material characterisation and on the side of RF measurements, to understand which kind of surface state could enhance the accelerating field inside the cavity. We used XPS and AES measurements to investigate the surface of different treated Nb samples, as these techniques allows to penetrate the first atomic layers of a surface without destroying it. Moreover the XPS and AES data contain information about the chemical states of the elements and about their in-depth distribution.

The surface treatments consist of different expositions to air and to dry O<sub>2</sub> to evaluate the content of Nb hydroxides. These oxides seems to prevent the achievement of high gradients in RF resonators. The encouraging results obtained by surface analysis (thinner and more uniform oxides, lower surface reactivity, lower carbon contamination, ...) convinced us to apply dry oxidation to a 3 GHz bulk Nb cavity, whose maximum accelerating fields were 20 MV/m after the usual surface treatments (deep chemical polishing, heat treatment, ...).

## 2 EXPERIMENTAL

The Nb samples were exposed for the same amounts of time to dry O<sub>2</sub> and to air at atmospheric pressure after a heat treatment, that was performed in a standard UHV furnace ( $T = 1500$  C,  $p \approx 1 \times 10^{-8}$  Torr).

The characterisation of the samples was made employing an XPS spectrometer and the RF measurements on a differently prepared cavity were performed by using a standard RF set-up.

### *2.1 Sample preparation*

The XPS sample is a bulk Nb cylinder (RRR  $\approx$  250) BCP treated to remove any trace of mechanical machining. We produced two series of samples: both were UHV fired and then one was exposed for different times to air at atmospheric pressure and the other to dry O<sub>2</sub> for the same amounts of time. This last treatment was performed inside the UHV furnace after the firing. Then

---

<sup>#</sup> E-mail: Renzo.Parodi@ge.infn.it

the samples were inserted into the XPS spectrometer for the characterisation of the surface.

## 2.2 Cavity preparation

To compare the effects of different surface treatments on the efficiency of a RF resonator, we measured the Q value vs. the accelerating field in a 3 GHz bulk Niobium cavity (RRR 250), after each treatment. The cavity is designed with  $\beta=1$ .

The cavity consists in two semicells built using deep drawing technique and joined together using electron beam welding (Zanon S.p.A.). The cavity diameter is 10 cm and the total length is 13 cm.

The construction includes the following steps: chemical polishing of the semicells in a 1:1:1 solution of phosphoric, nitric and fluoridric acid for 15 minutes, hot and then cold ultrapure water rinsing, nitrogen ventilation drying.

The welding is made by an electron beam in high vacuum ( $10^{-6}$  Torr) with a maximum energy of 2.89 KJ/cm. After the welding the cavity is washed with detergent liquids and rinsed with deionized water. Then another 20 seconds BCP treatments is made.

Inside the measurement apparatus the cavity is shielded with a  $\mu$ metal cylinder to avoid magnetic trapping during the cooling.

The measures of Q vs.  $E_{acc}$  were made after the following surface treatments:

- **light chemical polishing** consisting in one minute of BCP treatment followed by an ultrapure water rinsing.
- **deep chemical polishing** consisting in several 30 second lasting immersions of the cavity in the BCP solution, up to 200 microns surface layer were removed
- **UHV firing** for nine hours in ultra high vacuum baking ( $10^{-8}$  Torr) at 1950 C to remove surface impurities.
- **dry Nb<sub>2</sub>O<sub>5</sub> layer growth** consisting in a heat treatment followed by a long exposure to pure oxygen.

## 2.3 XPS spectrometer

The XPS and AES measurements were performed on a PHI ESCA 5600Ci Multitechnique spectrometer. The pressure inside the chamber was in the range  $2\text{-}5 \times 10^{-10}$  Torr and it was reached by using a combination of a rotary and turbomolecular pump (in the pre-pumping phase) and a ion and a titanium sublimation pump (for the UHV phase). The main components of the residual gas are detected by a RGA and are H<sub>2</sub> and H<sub>2</sub>O and, only in a minor quantity, CO, Ar and CO<sub>2</sub>. A detailed description of the entire system can be found in [1].

All measurements were realised by using the AlK $\alpha$  monochromatized source ( $h\nu = 1486.6$  eV) and the SCA (Spherical Capacitor Analyser) electron energy analyser in the FAT mode with a constant pass energy (187.85 eV for the low resolution spectra and 5.75 eV for the high resolution ones). The XPS analyses concern an area of 800  $\mu$ m of diameter with a take-off angle of 45° (the angle between the sample surface and the axis of the analyser) and an angular resolution of  $\pm 7^\circ$ . For the angle-resolved measurements we used a more precise lens that acquires the data on a 400  $\mu$ m of diameter area and with an angular resolution of  $\pm 2^\circ$ .

The first XPS characterisation consists in a wide spectra acquisition (about 1400 eV) to identify all the elements present on the surface (mainly Nb, O and C); then the high resolution acquisition allows to identify the chemical states of each element by operating a deconvolution on the spectra with a non-linear least square fitting method. In particular the Nb3d lines were reproduced by asymmetric Gaussian - Lorentzian functions [2]. To calculate the atomic concentrations of the elements identified we used the relation:

$$X_A = \frac{I_A/S_A}{\sum_{i=1}^N I_i/S_i} \quad (1)$$

where  $S_A$  is the sensitivity factor for the element A (the sensitivity factor for the F1s line is conventionally set to 1) and N is the number of elements identified on the surface.

The in-depth chemical composition of each sample was determined by ARXPS (Angle-Resolved XPS) analysis (a non destructive method), varying the take-off angle between 30° and 90°. The formula employed to calculate the thickness of a stack of oxides  $i$  on a substrate S (Nb) was the following [3]:

$$d_i = \lambda_i \sin\theta \cdot \ln \left( 1 + \frac{X_i}{X_S} T_2 T_3 \cdots T_{i-1} \right) \quad (2)$$

where  $\lambda_i$  is the attenuation length and  $T_i$  is the transmission coefficient of the  $i$ -th layer, given by:

$$T_i = \exp(-d_i/\lambda_i \sin\theta) \quad (3)$$

## 3 RESULTS

We present first the XPS - AES data and then the RF measurements, as we decided to apply the same surface treatments employed for the Nb samples to the RF cavity.

### 3.1 XPS and ARXPS measurements

The chemical elements identified on both the Nb sample series (exposed to air and to  $O_2$ ) by a low resolution XPS analysis were Nb, O and C. The deconvolution of the Nb3d line (reported in Figure 1) for one of the samples exposed to air allows to determine the presence of four chemical states: pure Nb ( $E_B=201.9$  eV), NbO ( $E_B=202.5$  eV), NbO<sub>2</sub> ( $E_B=204.0$  eV) and Nb<sub>2</sub>O<sub>5</sub> ( $E_B=207.5$  eV) [4]. The intensities of each spectra are reported on the ordinates in arbitrary units.

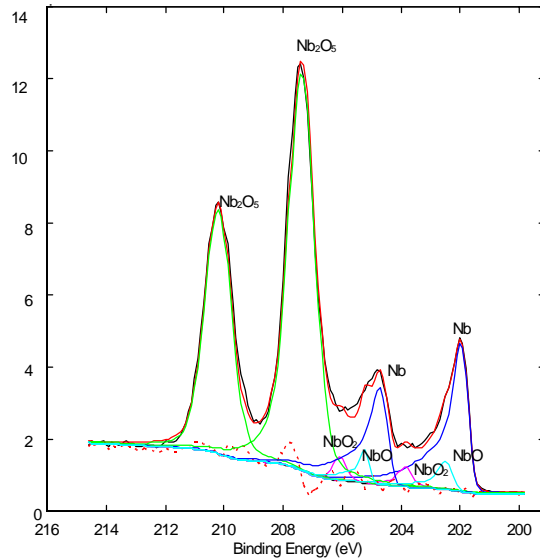


Figure 1 Deconvolution of the Nb3d line for one of the samples exposed to air; to reproduce the line-shape four chemical states (Nb, NbO, NbO<sub>2</sub>, Nb<sub>2</sub>O<sub>5</sub>) are necessary.

From the angle-resolved XPS measurements we were able to establish that upon the pure Nb there was a layer of NbO, followed by a layer of NbO<sub>2</sub> and then by a layer of Nb<sub>2</sub>O<sub>5</sub> of different thickness. Above this oxides stratification there is a layer of material coming from atmospheric contamination, whose nature is established from the deconvolution of the O1s and C1s lines.

In Figure 2 the O1s line of one of the samples exposed to air is reproduced by three chemical states: the signal at  $E_B=530.7$  eV produced by the Nb oxides, the peak at  $E_B=531.6$  eV coming from the C=O and C-OH bonds and the line at  $E_B=532.7$  eV generated by the OH present in the Nb hydroxides [4, 5, 6]. This last chemical state is more pronounced in the samples exposed to air than in the ones exposed to dry  $O_2$ , as shown in Figure 3.

The C1s line is produced by the superposition of three different peaks (Figure 4): the signal at  $E_B=285.2$  eV typical of graphite, the line at  $E_B=286.4$  eV attributed to the C-OH bond and the one at  $E_B=288.9$  eV identified as the C=O bond [4, 5].

According to the ARXPS analyses, the layer of carbon (including graphite and the C=O and C-OH adsorbates) is positioned above the Nb oxides layer and between these two layers there is a region occupied by the Nb hydroxides (whose thickness varies from 1-2 monolayers to a fraction of a layer).

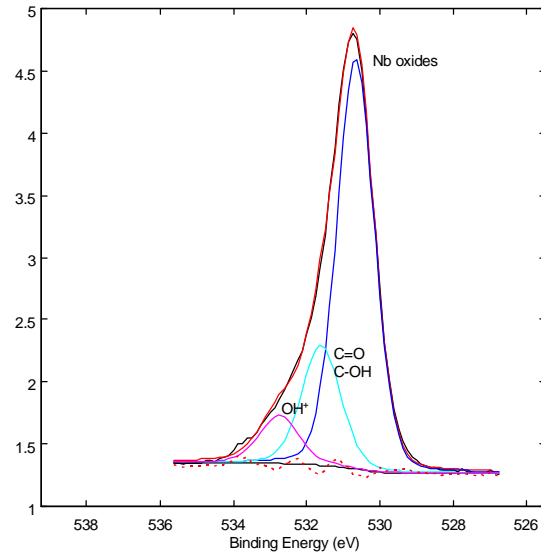


Figure 2 Deconvolution of the O1s line for one of the samples exposed to air; the spectrum is reproduced by three chemical states (Nb oxides, C=O and C-OH, OH<sup>+</sup>).

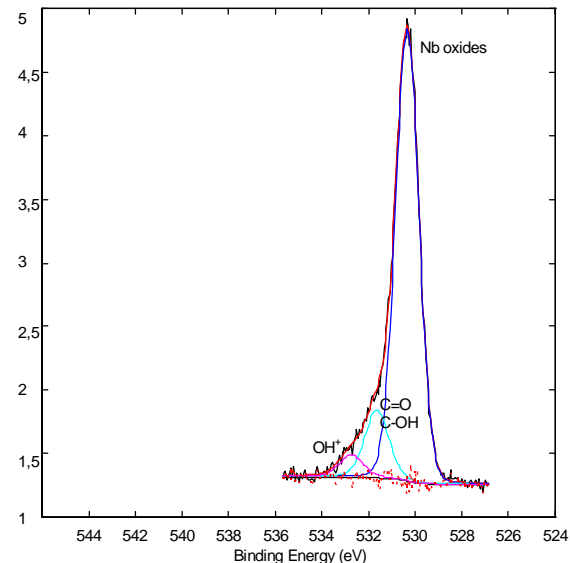


Figure 3 Deconvolution of the O1s line for one of the samples dry oxidised; the spectrum is reproduced by three chemical states as in Figure 2, but the contribution of the OH<sup>+</sup> signal is strongly reduced.

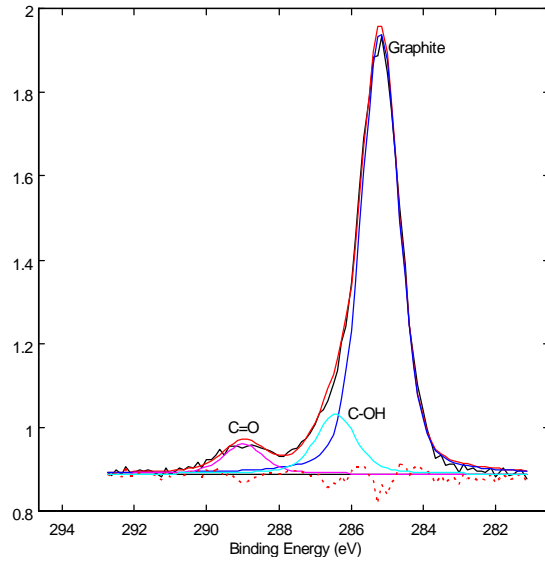


Figure 4 Deconvolution of the C1s line for one of the samples exposed to air; from the curve fitting we determine the presence of three chemical states (graphite, C-OH, C=O).

The in-depth chemical composition of the samples analysed is plotted in Figure 5: we have reported the stratification deduced from the ARXPS measurements for the samples exposed to air, for the ones exposed to dry  $O_2$  and for these last ones exposed for a long period (about 10 days) to air at atmospheric pressure after the first analysis. The error on the estimate of the thickness of each layer ranges between  $\pm 0.1$  and  $\pm 0.3$  monolayers.

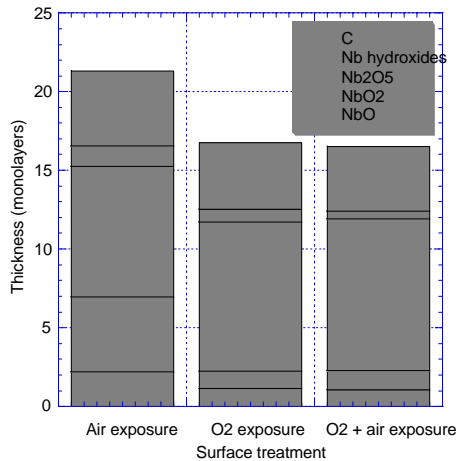


Figure 5 In-depth chemical composition of the samples exposed to air and to dry  $O_2$  (up to saturation). The last bar represents the in-depth composition of the dry oxidised samples exposed for a long time (about 10 days) to air after the dry  $O_2$  exposure. The errors on the thickness values are between  $\pm 0.1$  and  $\pm 0.3$  monolayers.

It is evident from Figure 5 that the total thickness of the oxides layer for the samples exposed to dry  $O_2$  is thinner than for the ones exposed to air; the thickness of the lower oxides ( $NbO$  and  $NbO_2$ ) is reduced for the second samples and, consequently, almost all the oxides layer is made up of  $Nb_2O_5$ . The samples exposed to air, instead, are richer in lower oxides, having enhanced losses in RF fields. We also performed some measurements of the work function ( $\Phi$ ) (by using the XPS spectrometer [7]) and we found that the samples exposed to air show a lower value of  $\Phi$  (about 3.8 - 4.4 eV) with respect to the dry oxidised ones ( $\Phi \cong 4.9 - 5.2$  eV). Lower values of  $\Phi$  enhance the electron emission process, according to the Fowler and Nordheim law [8].

A further exposure to air, also for a long time, of the dry oxidised samples do not increase the thickness of the contaminant layers (the oxides and the carbon layers) as shown in Figure 5: the total thickness values stay constant within the experimental errors.

The AES measurements confirm the chemical characterisation obtained by XPS.

### 3.2 RF measurements

We report below the results of the different measurements of the Q factor vs. the accelerating field, after each surface treatment.

The plots are a selection of the several test made for any treatment.

In all measurements, the maximum value obtained for the accelerating field corresponds to the highest value of the power injected in the cavity before the quench, apart the ones followed by the new oxidation treatment in which we did not observe any thermal breakdown. The temperature, at which the measurements were done, was the lowest reachable by our cooling system. Its value is about 1.5~1.8 K kept almost constant during each measurement.

The cavity underwent first a chemical polishing with a BCP acid solution for one minute. The Niobium surface is so rinsed in ultra pure water and mounted in a 100 class clean room.

As shown in Figure 6, under these surface conditions, the maximum Q value reaches  $10^8$ , and the accelerating field cannot go over 8 MV/m. The peak values of electric and magnetic fields are respectively: 17 MV/m and 28 mT.

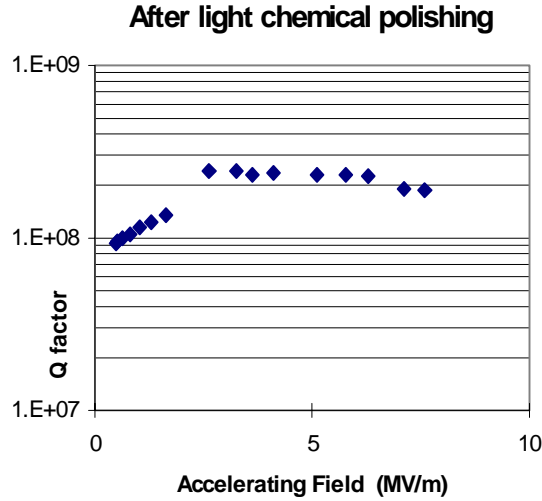


Figure 6: plot of Q factor vs. accelerating field after one minute of BCP treatment

By several immersions of the cavity in the BCP acid solution, a 200 microns surface layer was removed. This deeper chemical polishing eliminate the microscopic defects and the impurities, due to the high reactivity of Niobium to oxygen and hydrogen, present especially just under the surface. The results are reported in Figure 7. The efficiency improvement of the cavity, after the treatment, is shown by a Q factor three times higher then the previous one with an accelerating field that reaches 18 MV/m. Increasing the injected power, above the value corresponding to this field, an RF breakdown occurs.

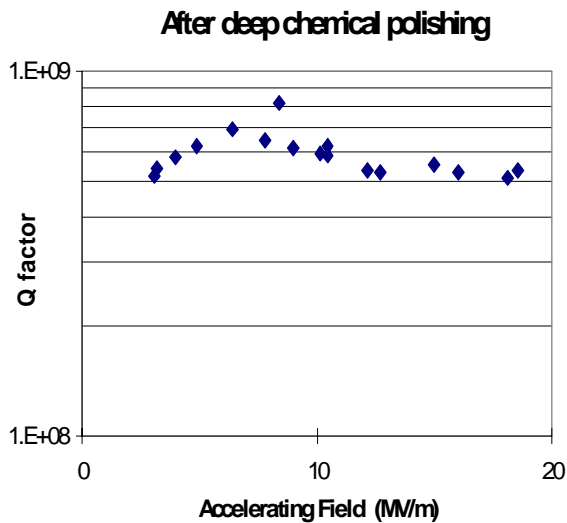


Figure 7: plot of Q factor vs. accelerating field after the removal of 200 microns surface layer.

Thermal treatments improve further SRF resonators performance, allowing the degassing of inner impurities from the cavity's walls. After 9 hours of baking, at the temperature of 1950 C and at the pressure of  $10^{-8}$  Torr, the Q factor, as Figure 8 shows, goes over  $10^9$  and the corresponding accelerating field over 20 MV/m.

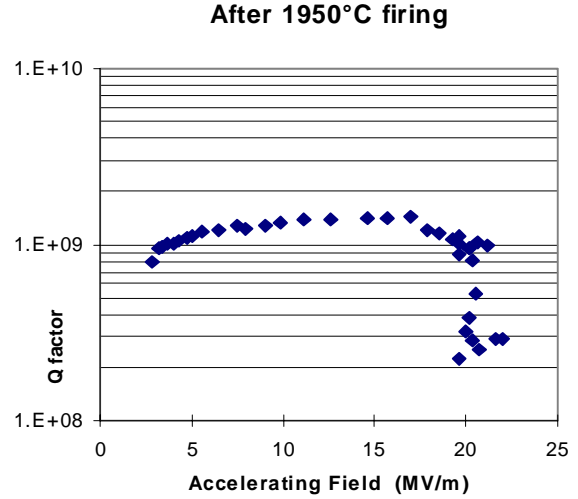


Figure 8: plot of Q factor vs. accelerating field after nine hours of baking.

At the maximum reachable field, is now possible to increase the power before the quench. According to the relation  $E_{acc} = 240\sqrt{P_{diss}Q_0}$ , calculated by

OSCAR 2D program [9], the maximum accelerating field remains at its highest value while injected power increases. In this situation the physical process that cuts off the RF performance is the electron loading.

The treatments we reported are considered standard ones. The values obtained during our measurements reproduce and confirm the validity of these methods already tested in other laboratories. [10, 11, 12]

As discussed in the previous paragraph, XPS analyses on Nb samples, investigating their superficial structure after a long exposure to oxygen, suggested a new oxidation technique that provides the growth of thinner  $Nb_2O_5$  layer and reduces the harmful hydroxides layer.

The application of this treatment to our cavity gave the results shown in Figure 9. During the measure an HPP treatment was made.

Now the Q factor is about  $5 \times 10^9$  and the limiting accelerating field increases to 32 MV/m. The points plotted in the right part of the graph refer to the RF conditioning (HPP). We repeated the measure in the same conditions obtaining the results plotted in Figure 10.

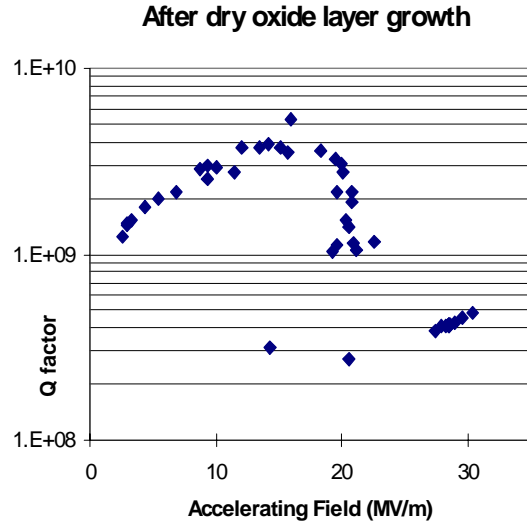


Figure 9: plot of Q factor vs. accelerating field after dry oxidation; the data in the right part of the plot were obtained during HPP treatment.

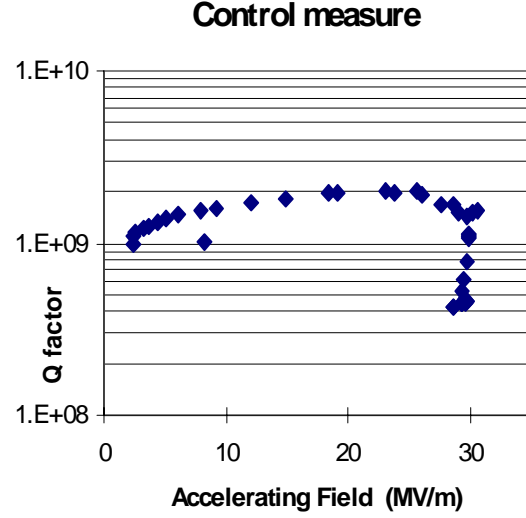


Figure 11: plot of Q factor vs. accelerating field after dry oxidation. The measure was made several days after the first one.

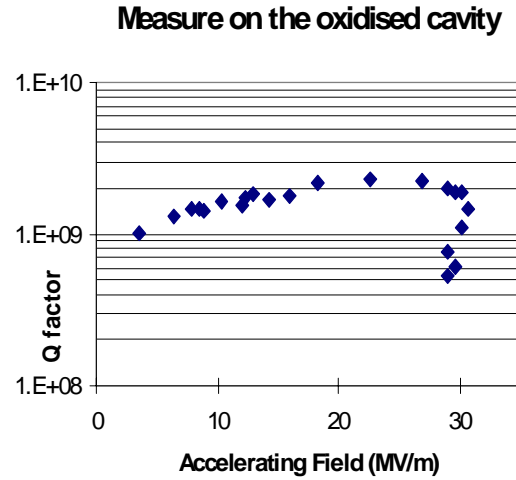


Figure 10: plot of Q factor vs. accelerating field after dry oxidation and HPP treatment.

Also in this case we observe no quench. A surface heating is responsible of low Q values at high fields but no electrons were detected. Several control measurements repeated after many days, one is shown in Figure 11, reveal no appreciable changes in RF performances.

Further HPP treatments did not improve RF efficiency confirming that electron loading was strongly cut off. The values of the Q factor and of the fields, measured after each treatment, are reported in the Table 1.

Treatment	Chemical (Light)	Chemical (Deep)	Thermal	Oxidation
$Q_0$	$2 \cdot 10^8$	$5/6 \cdot 10^8$	$1.05 \cdot 10^9$	$4/5 \cdot 10^9$
Eacc (MV/m)	8	18	22	30
Epeak (MV/m)	17	40	45	65
Hpeak (mT)	28	68	75	110
$R_s (\Omega)$	$2.5 \cdot 10^{-6}$	$4.5 \cdot 10^{-7}$	$1.8 \cdot 10^{-7}$	$6.8 \cdot 10^{-8}$

Table 1: Summary of the performances related to the various treatments

## 4 DISCUSSION

The results obtained from the XPS analyses confirm the hypothesis that dry oxidation strongly reduces (up to about 50%) the presence of Nb hydroxides on Nb surface. Moreover we found that the oxides layer grown on the surface after this treatment consists mainly of  $Nb_2O_5$ , while the thickness of the lower oxides ( $NbO$  and  $NbO_2$ ) is thinner than the ones measured for the Nb samples exposed to air. Also the carbon layer upon the oxides shows a reduced thickness in the case of dry  $O_2$  exposure, even if these XPS measurements suffer of the contamination produced by air during the transportation from the furnace (inside which the dry oxidation took place) to the XPS spectrometer.

Another important result comes from the measurements performed on the dry oxidised samples that were

maintained in air even for long times after the treatment: the chemical composition of the surface layers and the thickness of the different compound remain unchanged within the experimental errors. Therefore dry oxidation produces a less reactive surface, passivating the external layers.

The XPS and ARXPS measurements show that the oxides layer grown in dry O<sub>2</sub> is thinner and more uniform, while the air oxidation produces a more porous surface layer that probably allows the oxygen atoms to migrate under the oxides layer and to react with pure Nb, enhancing the surface reactivity. These results induced us to apply this new surface treatment to RF cavities, to verify if these improved surface quality could effectively enhance the RF performances of our resonators.

The comparison of the Q value and of the fields we measured inside the 3 GHz cavity, show a great RF efficiency enhancement after dry oxidation respect to the conventional surface treatments.

The accelerating field increases of about the 45% respect to the thermal treatment, that is the best among the conventional ones, and the Q factor, from 10<sup>9</sup>, reaches 5x10<sup>9</sup>.

The measurements confirm also that thermal treatment is more effective than the chemical one but in both cases we observed a thermal breakdown increasing the injected power.

After dry oxidation there was no quench even at the maximum value of power delivered by our RF generator (20 W), allowing a high power processing that further improved the RF performance.

The error in our measurements, due to the intrinsic characteristics of the apparatus, is 5%.

No measurable electron loading was measured in dry oxygen treated cavities confirming that stable, dry and compact layers of Nb<sub>2</sub>O<sub>5</sub>, built up with this new technique, are effective in lowering the sticking coefficient of extraneous molecules and in cutting off the non resonant electronic emission as the result of the increasing of the work function.

## 5 CONCLUSIONS

A surface treatment for RF cavities was suggested from the results obtained on differently oxidised Nb samples. XPS and AES measurements show that dry oxidation after a standard heat treatment produces thinner and more uniform oxides, reducing the content of Nb hydroxides, NbO, NbO<sub>2</sub> and carbon, that are always present on an air oxidised surface. The O<sub>2</sub> exposure lowers the surface reactivity and passivate it also for long periods of time. Applying the same treatment to a 3GHz bulk Nb cavity we observe an increase in the accelerating field of about 45%. The Nb cavities UHV fired show a maximum field of 20 MV/m but were limited by a strong NREL. The dry oxidation after a

UHV firing increases the limiting field to 32 MV/m without producing any detectable electron loading.

## 6 REFERENCES

- 1 A. Daccà, G. Gemme, L. Mattera, R. Parodi, *Appl. Surf. Sci.*, **126**, 219, (1998).
- 2 M. Cardona, L. Ley, "Photoemission in Solid I", Springer, (1978).
- 3 A. Darlinski, J. Halbritter, *J. Vac. Sci. Technol. A* **5** (4), 1235 (1987).
- 4 J. F. Moulder, W. F. Stickle, P. E. Sobol, K. D. Bomben, "Handbook of X-ray Photoelectron Spectroscopy", J. Chastain editor, Perkin - Elmer Corporation, Physical Electronics Division, USA, (1992).
- 5 M. P. Seah, J. H. Qiu, P. J. Cumpson, J. E. Castle, *Surf. Interface Anal.*, **21**, 336 (1994).
- 6 M. Grunder, J. Halbritter, *J. Appl. Phys.*, **51** (10), 5396, (1980).
- 7 A. Daccà, G. Gemme, L. Mattera, R. Parodi, *Particle Accelerators*, **60**, 103, (1998).
- 8 R. H. Fowler, L. Nordheim, *Proc. of Royal Society*, **119**, 173 (1928).
- 9 P. Fernandez, R. Parodi, "OSCAR 2D User's Guide", INFN/TC-90/04, (1990).
- 10 H. Padamsee et al., "New Results on RF and DC Field Emission", *Proc. of 4<sup>th</sup> Workshop. on RF Superconductivity*, Y. Kojima ed., KEK, Tsukuba, (1989).
- 11 P. Kneisel, "Surface Preparation of Niobium" *Proc. of the Workshop on RF Superconductivity*, M. Kuntze ed., Karlsruhe, (1980).
- 12 P. Kneisel, "Effect of Cavity Vacuum on Performance of Supercond. Niobium Cavities", *Proc. of the 7<sup>th</sup> Workshop on RF Superconductivity*, B. Bonin ed., Gif sur Yvette, (1995).